



Small emission sources disproportionately account for a large majority of total methane emissions from the US oil and gas sector

5 James P. Williams¹, Mark Omara^{1,2}, Anthony Himmelberger², Daniel Zavala-Araiza¹, Katlyn MacKay¹, Joshua Benmergui^{1,2,3}, Maryann Sargent³, Steven C. Wofsy³, Steven P. Hamburg^{1,2}, Ritesh Gautam^{1,2}

¹Environmental Defense Fund, New York, NY, USA 10010

²MethaneSAT, LLC, Austin, TX, USA 78701

³Harvard University, Cambridge, MA, USA 02138

10

Correspondence to: James P. Williams (jamwilliams@edf.org), Ritesh Gautam (rgautam@edf.org)

15

Abstract. Reducing methane emissions from the oil and gas (oil/gas) sector has been identified as a critically important global strategy for reducing near-term climate warming. Recent measurements, especially by satellite and aerial remote sensing, underscore the importance of targeting the small number of facilities emitting methane at high rates (i.e., “super-emitters”) for measurement and mitigation. However, the contributions from individual oil/gas facilities emitting at low emission rates that are often undetected are poorly understood, especially in the context of total national- and regional-level estimates. In this work, we compile empirical measurements gathered using methods with low limits of detection to develop a facility-level model to quantify total methane emissions from the continental United States (CONUS) midstream and upstream oil/gas sector for 2021. We find that ~70% (95% confidence intervals: 63-82%) of total oil/gas methane emissions in the CONUS for the year 2021 (Total: 14.3 Tg/yr) originate from facilities emitting <100 kg/hr. While there is variability among the emission distribution curves for different oil/gas production basins, facilities with low emissions are consistently found to account for the majority of total basin emissions (i.e., range across basins 63% - 90% of total basin emissions from facilities emitting <100 kg/hr). Production well sites were responsible for 70% of total regional oil/gas methane emissions, with the highest contributions from a large population of low-producing well sites. Our results are also in broad agreement with several independent aerial remote sensing campaigns (e.g., MethaneAIR, Bridger Gas Mapping LiDAR, AVIRIS-NG, and Global Airborne Observatory). Our findings highlight the importance of accounting for the significant contribution of small emission sources to total oil/gas methane emissions. While reducing emissions from high-emitting facilities is important, it is not sufficient for the overall mitigation of methane emissions from the oil and gas sector which according to this study is dominated by small emission sources across the US. Tracking changes in emissions over time and designing effective mitigation policies should consider the large contribution of small methane sources to total emissions.

20
25
30
35



1 Introduction

40 Methane is a short-lived but powerful greenhouse gas with a global warming potential more than 80 times
stronger than carbon dioxide (CO₂) over 20 years (AR6 Synthesis Report: Climate Change 2023, 2024). Therefore,
the reduction of methane emissions has become a key goal to achieve rapid climate mitigation in the short term
(Oeko et al., 2021). In North America, one of the largest sources of methane emissions originates from the oil and
gas (oil/gas) sector, with most emissions originating from the production (i.e., upstream) and transportation/storage
45 (i.e., midstream) sectors (Alvarez et al., 2018). Multiple studies, especially over the past decade, have focused on the
quantification of methane sources from the oil/gas sector, with particular emphasis on the continental United States
(CONUS) (Alvarez et al., 2018; de Gouw et al., 2020; Omara et al., 2018; Lu et al., 2022; Zhang et al., 2020; Shen
et al., 2022; Cusworth et al., 2022; Nesser et al., 2023; Brandt et al., 2016; Duren et al., 2019; Maasackers et al.,
2021; Lu et al., 2023; Worden et al., 2022). Several studies have recognized the importance of a small percentage of
50 high-emitting sites (i.e. “super-emitters”) and reported them as accounting for a large fraction of total methane
emissions (Cusworth et al., 2022; Brandt et al., 2016; Duren et al., 2019; Sherwin et al., 2024). Emissions from
oil/gas sites have been captured with greater frequency with advances in aerial and satellite remote sensing
technologies that allow for mapping wide areas faster, further emphasizing the importance of the remote sensing
approach. Despite the improved ability to locate and quantify emissions from high-emitting sites, there has been
55 considerable lack of understanding about the characteristics of low methane emitting facilities, especially those
emitting at rates below the limits of detection (LOD) of most point-source detection remote sensing platforms, and
their contributions to total oil/gas methane emissions.

While some studies offer important yet limited insights into the contributions of different lower-emitting
infrastructure from the CONUS oil/gas sector, there is a lack of understanding about their overall contribution to the
60 total sectoral regional and national scale emissions. A recent study by Xia et al. (2024) combined aerial remote
sensing data from Bridger Gas Mapping LiDAR (Bridger GML) in four oil/gas basins supplemented with
component-level modeling for facilities emitting below the Bridger GML LOD and found significantly more
emission sources in the 1 – 10 kg/hr range when compared to the emission distribution used by the EPA (Xia et al.,
2024). In a study focused on production well sites in the CONUS, the main source of methane emissions from the
65 oil/gas sector (Alvarez et al., 2018; Omara et al., 2018; Rutherford et al., 2021), Omara et al. (2018) found that 90%
of total methane emissions from producing well sites came from those emitting at rates <100 kg/hr. A follow-up
study by Omara et al. (2022) highlights that the total methane emissions from low-producing well sites producing
less than 15 barrels of oil equivalent per day (boed), which comprise 80% of all producing well sites in the CONUS,
were responsible for nearly half of all methane emissions from the oil/gas production sector. Kunkel et al. (2023)
70 observed that the use of Bridger GML combined with prior Carbon Mapper detections in a section of the Permian
basin showed a significant contribution from sources below the listed LOD of Carbon Mapper of 10 kg/hr. Cusworth
et al. (2022) found that 35% of total methane emissions (including non-oil/gas sources) from several major oil/gas
producing basins (other than the Appalachian basin) in the CONUS come from facilities emitting >10 kg/hr,
indicating that 65% of emissions come from facilities emitting <10 kg/hr. Although these studies using independent



75 measurement platforms provide new emerging insights about the importance of low methane emitting oil/gas
facilities, there generally remains a lack of quantitative assessment of the relative fractions of emissions originating
from different emission rate thresholds aggregated over individual oil/gas basins as well as at a national scale.

There are a variety of different methane quantification methods that differ in terms of their spatial resolution of
sources, logistical constraints, costs of implementation, and their LODs. Measurement method sensitivities and
80 LODs have important policy implications. For example, the Environmental Protection Agency (EPA) recently
finalized regulations that define a “super-emitter event” as an emission rate threshold of 100 kg/hr or greater (EPA’s
Final Rule for Oil and Natural Gas Operations Will Sharply Reduce Methane and Other Harmful Pollution., 2024),
albeit without clear information on what percentage of total regional emissions are captured within this definition.
Satellite and aerial remote sensing methods have point source LODs that range anywhere from 1-3 kg/hr for
85 Bridger’s airborne GML (Kunkel et al., 2023; Johnson et al., 2021; Thorpe et al., 2024; Xia et al., 2024) to ~200
kg/hr for GHGSat (Sherwin et al., 2023). In contrast, ground-based measurement methods such as OTM-33a and
tracer release have LODs <1 kg/hr (Fox et al., 2019). A study by Ravikumar et al. (2018) using the Fugitive
Emissions Abatement Simulation Toolkit (FEAST) suggests that a method with a LOD of 0.1-1 kg/hr would
sufficiently capture all emissions from the oil/gas sector, whereas the ability to quantify emissions below this
90 threshold would not lead to any significant increases in mitigation. Ultimately, there is a need for clarification in the
total percentage contribution of emissions originating from a given emission rate threshold, which requires
characterizing entire emissions distributions, not only the high emitters.

In this work, we create and analyze measurement-based methane emission rate distributions of US upstream and
midstream oil/gas facilities to determine the percentage contributions of different emission rate thresholds to total
95 methane emissions. First, we use empirical measurements gathered from ground-based sampling platforms to
develop a bottom-up facility-based model to estimate methane emissions for upstream and midstream facilities in
the continental US (CONUS) for 2021. Next, we aggregate our facility-level, population-based data to determine the
national- and basin-level contributions of methane emissions originating from facilities emitting at different
emission rate thresholds, in addition to comparisons to aerial-remote sensing platforms. Finally, we break down the
100 emission distribution curves by facility category to analyze how the percentage contributions of total emissions vary
across facility types.

2 Materials and methods

105 2.1 Empirical measurements

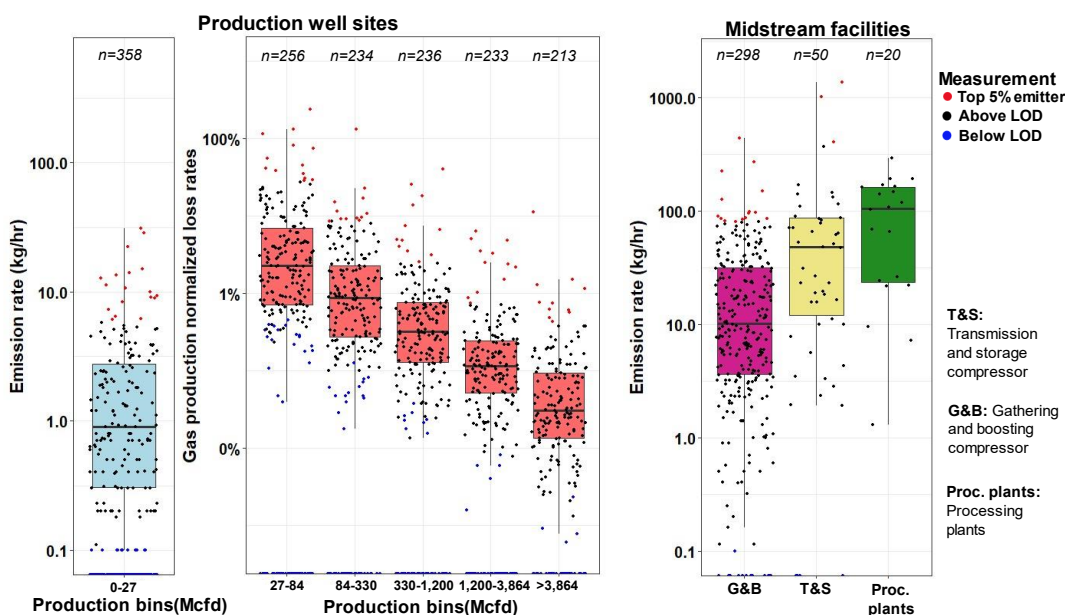
We compile 1,898 facility-level methane emission rate measurements from 13 studies (Caulton et al., 2019;
Brantley et al., 2014; Deighton et al., 2020; Omara et al., 2016; Rella et al., 2015; Riddick et al., 2019; Robertson et
al., 2017, 2020; Zhou et al., 2021; Zimmerle et al., 2020; Mitchell et al., 2015; Subramanian et al., 2015) that use



110 ground-based site/facility level and source/component level measurement methods with low LOD's of ~0.1 kg/hr.
85% of empirical measurements we use in this work were gathered using ground-based mobile laboratories that
quantified methane emissions at the site/facility level using either tracer-based releases, the EPA Other Test Method
(OTM-33a), or Gaussian plume transport modeling (Fox et al., 2019) (Table S1). From the remaining empirical
measurements we use (i.e., 15%), measurements from three studies (Riddick et al., 2019; Deighton et al., 2020;
115 Zimmerle et al., 2020) used ground-based methods that aggregated source/component-level HiFlow sampling or
static/dynamic chamber measurements, which could mean that other on-site emission sources were not quantified
during measurement and overall emission rate estimates are conservative.

The compiled empirical measurements target a variety of production well sites and/or midstream facilities
across at least nine oil/gas-producing basins in the CONUS (Table S2). For all facility categories (i.e., compressor
120 stations, processing plants, production well sites), we prioritize datasets of randomly sampled sites that include
measurements below the method's LOD or reported as zero emissions, except for measurements from two studies
(Brantley et al., 2014; Lan et al., 2015) which we discuss later in Section 2.3. Additionally, for production well site
measurements, we focus only on data that provide facility-level gas production data for the date/month of
measurement. Our compiled dataset of measurements includes both routine intentional (e.g., venting from pneumatic
125 devices) and non-intentional (e.g., malfunctioning equipment) emissions, and while we remove any measurements
attributed to high emitting intermittent events such as flowbacks and liquids unloadings if that information is
present, we cannot fully discount that emissions from these high-emitting intermittent are included in our compiled
dataset. Furthermore, we remove any empirical measurement data associated with flaring emissions, which are
discussed below, if that information is provided in the empirical data.

130 We categorize the empirical measurements by facility category as production well sites, gathering and boosting
compressor stations (G&B compressors), transmission and storage compressor stations (T&S compressors), or
processing plants. We group the empirical measurements from production well sites into six production bins based
on gross average daily gas production as reported in individual studies. We use gross daily average gas production
data instead of oil and gas production data for two reasons: 1) the limited availability of facility-level oil production
135 data provided from empirical measurements; and 2) the established relationship between gas production and
emission rates observed in previous work (Omara et al., 2018, 2022, 2024a). The gas production ranges of the
production bins (Fig. 1) are chosen to evenly distribute empirical measurements above the method LOD to all six
production bins. This categorization creates nine distinct facility categories: G&B compressors, T&S compressors,
processing plants, and six groups of production well sites. We further classify the nine distinct facility categories
140 into five primary facility categories: low-production well sites which produce combined oil and gas <15 boed, non-
low-producing well sites which produce ≥ 15 boed, processing plants, G&B compressors, and T&S compressors. In
addition to these facility categorizations, we also include Visible Infrared Imaging Radiometer Suite (VIIRS) flare
detections in our analysis, which are treated as an independent methane source since flares can be located on
multiple facility categories across the upstream and midstream oil/gas sectors.



145

150

Figure 1: Facility-level empirical measurement data distributed by different distinct facility categories for production well sites (left) and midstream facilities (right). Individual measurements are shown for each box plot and colored according to their emission rate status for that facility category, where blue points are considered non-detectable emissions below an emission rate threshold of ≤ 0.1 kg/hr/facility which is the method LOD we use, black points are measurements above our method LOD but below the top 5% emitter category, and red points are the top 5% of empirical emission rates for that facility category. The number of empirical measurements available for each facility category is denoted at the top of each boxplot. We show emission rates rather than loss rates for the lowest cohort of production well sites due to the reasoning presented in Section 2.3.

Mcfcd = thousands of cubic feet of gas per day, Proc. Plants = processing plants, G&B = gathering and boosting compressor station, T&S = transmission and storage compressor station, LOD = limit of detection.

155

2.2 Activity data

160

We use activity data (i.e., number of facilities and spatial locations) for actively producing wells in 2021 provided by Enverus for the CONUS. We calculate both the annual averaged daily gross gas production, and oil and gas production for each producing well using the number of producing days and total annual oil and gas production data provided by Enverus. We convert production wells to production well sites by spatially aggregating individual wells within 25-meter (vertical wells) or 50-meter (horizontal wells) distances from each other and merging their combined oil and gas production in boed and gas production in thousand cubic feet per day (Mcfcd), similar to previous approaches (Omara et al., 2018).

165

We acquire activity data for operational transmission and storage (T&S) and gathering and boosting (G&B) compressor stations and processing plants from Enverus for 2021 for the CONUS, which was further supplemented by additional data from the Oil and Gas Infrastructure Mapping (OGIM) database published in Omara et al. (2023). We filter data for these midstream facilities to include only active facilities in the year 2021. For VIIRS flare



170 detections, we use the 2021 natural gas flared volume estimates (Elvidge et al., 2016) based on natural gas flaring
detections provided by the VIIRS instruments installed aboard satellite platforms which have a 750x750 meter
source resolution (NOAA-20 and Suomi National Polar-orbiting Partnership) (Elvidge et al., 2017). In terms of
potential double-counting between the VIIRS flare detections and the empirical measurements we use in this work,
the majority of VIIRS detections are in the Permian, Bakken, and Eagle Ford oil/gas basins (i.e., 86% of total VIIRS
detections) which corresponds to a small number of our empirical measurement data (Table S2) (Plant et al., 2022).
175 However, the limited availability of spatial coordinates for our empirical measurements restricts our ability to
perform a direct comparison to exclude overlapping/proximal VIIRS detections and our facility-level empirical
measurements. Therefore, we do acknowledge that there is a possibility of double counting between our empirical
measurement data and the VIIRS flare detections, but we expect the degree of overlap to be low.

2.3 Facility-level methane emission inventory

180 We calculate annual methane emissions from all facility categories (i.e., six production bins of production well
sites, T&S compressor stations, G&B compressor stations, and processing plants) using a multi-step probabilistic
modeling approach adapted from Omara et al. (2018) (Fig. 2). For the highest five gas production bins of producing
well sites ranging from 27 – 3,864 Mcfd (or 4.5 - >644 boed), we use gross gas production normalized loss rates to
model the distributions used to calculate methane emission rates from Eq. (1), where the: *Loss rate* is the fraction of
185 emitted gas relative to gas production, CH_4 is the methane composition of the emitted gas (i.e., which we assume to
be 80%), and $\rho(CH_4)$ is the density of methane at 15°C and 101.325 kPa of 0.678 kg/m³. For the lowest well site
production bin (i.e., 0 – 27 Mcfd) and midstream facilities, we use the empirical absolute methane emission rate data
as is. This approach is partly based on the methods used by Omara et al. (2020) for the non-low production well site
category, which exploits a weak relationship between gross gas production data (which is most accessible in
190 empirical measurement studies) and emission rates to better extrapolate emissions to the entire population of
production well sites in the CONUS.

$$Emission\ rate\ \left[\frac{kg}{hr}\right] = Loss\ rate \times Gas\ production\ \left[\frac{Mcf}{day}\right] \times \frac{1000\ [cf^3]}{1\ [Mcf]} \times \frac{1\ [day]}{24\ [hr]} \times CH_4 \times \frac{0.0283\ [m^3]}{1\ [cf^3]} \times \rho(CH_4) \quad (1)$$

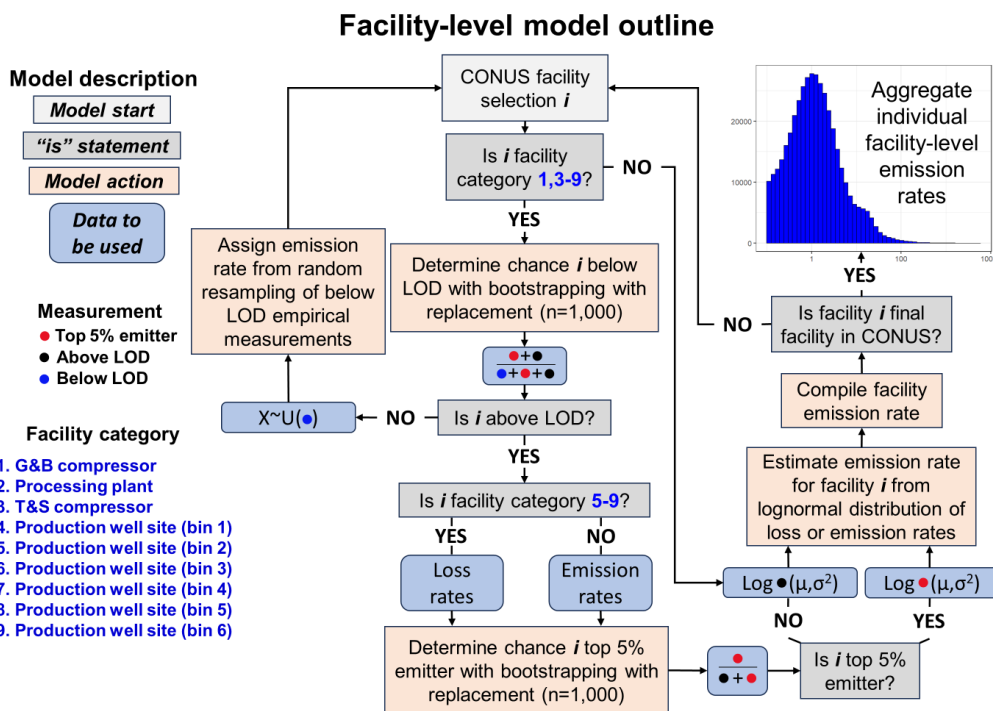
For our estimation of facility-level emission rates, we break down the modeling process into two separate steps:
the first determines whether a randomly selected facility is emitting methane above our method LOD of ≤ 0.1
195 kg/hr/facility, and the second determines the associated methane emission rate for that individual facility. To test the
sensitivity of our method to the selection of the method LOD, we also perform an additional sensitivity analysis for
other method LODs (Fig. S11-13). The processes outlined below are all specific to each of our nine facility
categories. Measurements from Brantley et al. (2014) and Lan et al. (2015) are excluded from this first step since
they do not include measurements below the method LOD but do include valuable data on well site emission rates
200 with associated well site production data. To determine whether a facility is emitting methane above the method
LOD threshold in our estimates, we first use bootstrapping with replacement (n=1,000) of our empirical
measurement data to determine the chance of an individual facility emitting methane above the method LOD (i.e.,



205 ≤ 0.1 kg/hr/facility), which we call an “emitting facility” or “emitter” herein (Fig. 2). We model the results of the bootstrapping with replacement as a normal distribution and use the parameters of the modeled distribution to randomly determine whether a facility is emitting. Next, we remove the empirical measurements below the LOD and use bootstrapping with replacement ($n=1,000$) on the above LOD empirical measurements to determine the probability of an emitting facility being in the top 5% (i.e., 95th percentile or above of empirical measurement data) or bottom 95% (i.e., 95th percentile or below the empirical measurement data) of emitters, except for processing plants which had too few measurements ($n=20$) to distinguish between the top 5% and bottom 95% of emission or loss rates. We fit the results of the bootstrapping to two normal distributions: one for the top 5% of emitters and one for the bottom 95% of emitters. We use the associated parameters of each normal distribution to randomly determine whether a facility is emitting in the top 5% or bottom 95% of emitters. These steps are repeated for each facility for each facility category in the CONUS.

215 At the end of the first step of this facility-level modeling process, all facilities in the CONUS are classified as either a: bottom 95% emitter, top 5% emitter, or below the method LOD. For facilities classified as the top 5% and bottom 95% of emitters, we estimate their methane emissions by first fitting a lognormal distribution to the empirical measurement data, including measurements from Brantley et al. (2014) and Lan et al. (2015), of either the gas production normalized loss rates or methane emission rates (Eq. 1), depending on the facility category. Next, we use the parameters of the modeled distributions to randomly assign either an emission or loss rate to a randomly selected facility ($n=500$), depending on its emitter status and facility category. We test each estimated methane emission distribution to the associated empirical measurements and find a good fit for all facility categories (Table S5). To account for facilities emitting below the method LOD, we randomly assign an emission rate from re-sampling our dataset of empirical measurements below the method LOD for that facility category. Finally, once all facilities are assigned an emission rate, we compile the ensemble of emission distributions to develop facility-level emission distribution curves and total regional oil/gas methane emissions for the CONUS in 2021.

230 For all VIIRS flares detections, we use the total reported volumes of gas flared for 2021 by Elvidge et al. (2016) multiplied by the flaring combustion efficiencies from Plant et al. (2022) to calculate annual methane emission rates from this source. As previously stated, our empirical measurements are largely located outside of oil/gas basins (i.e. Permian, Eagle Ford, and Bakken) where the majority of VIIRS flare detections are located, but we cannot discount the possibility that there are instances of double-counting flares measured via our ground-based empirical data and those detected by VIIRS. We model flaring combustion efficiencies as a normal distribution using the probability distribution parameters for the Bakken, Eagle Ford, and Permian basins (Plant et al., 2022). For areas outside of these basins, we used the total CONUS averaged flaring efficiencies as reported by Plant et al. (2022) of 91.1% (95% confidence interval: 90.2 – 91.8%).



235

Figure 2: Flowchart of the facility-level estimates, with steps colored according to the specific process and data being used. The methods used for estimating methane emissions from VIIRS flare detections are not shown here but are presented in the Methods section.

240 **2.4 Extrapolation to smaller spatial boundaries**

We perform several comparisons of our estimated emission distribution curves and total aggregated emissions to estimates from aerial and satellite remote-sensing studies. For comparisons to satellite remote-sensing studies, we prioritize national-level satellite inversions that estimate methane emissions from the CONUS that include spatially explicit maps of methane emission inversions specifically for oil/gas sources. We join the spatially explicit satellite inversions of methane emissions to the top twelve producing oil/gas basin boundaries in the CONUS, in addition to their national-level inversions which we also use for national comparisons. Since our facility-level model includes geo-located activity data (i.e., facility coordinates), we can estimate facility-level methane emissions distributions and estimate total methane emissions for any spatial boundary in the CONUS by spatially joining facilities within a target boundary. Spatial variability in our facility-level estimates is driven by two main factors: counts of facilities and facility types, and averaged annual production characteristics. Due to constraints on data availability, we do not constrain our available empirical measurement data to the specific regions where they were gathered (Table S2). We do note that basin-to-basin comparisons of the empirical measurement



255 data for production well sites that we use in this work generally do not show significant variations throughout the
well site production bins, with some exceptions (Fig. S3-S8). Due to a lack of data availability, we do not have
sufficient spatial information from empirical measurements of G&B compressors, T&S compressors, and processing
plants to test for basin-level differences in empirical measurement data.

260 For comparisons to aerial remote sensing studies/results, we prioritize studies that include both measured
point sources (i.e., oil/gas methane sources that are above the LOD of the aerial remote sensing measurement
platform), estimates of total regional oil/gas emissions, and descriptions/outlines of the surveyed spatial domains
which are required for these comparisons. Based on these criteria, we compare our estimated emissions to those
from three peer-reviewed studies (Kunkel et al., 2023; Xia et al., 2024; Cusworth et al., 2022) and the results of
research flights from MethaneAIR in the Permian and Uinta oil/gas basins (Omara et al., 2024; Chan Miller et al.,
2023; Chulakadabba et al., 2023; MethaneAIR, 2024). In all cases, we estimate facility-level methane
265 within the spatial domains outlined by the aerial remote sensing studies to estimate region-specific methane
emission distribution curves. We compare our spatially-joined facility-level emission distributions to the percentage
of emissions contributed from facilities emitting below discrete methane emission rate thresholds for all four aerial
remote sensing studies, and to the continuous cumulative methane emissions distribution curves from Bridger GML
surveys (Xia et al., 2024; Kunkel et al., 2023).

270 Each aerial remote sensing campaign utilizes independent methods to estimate their percentage
contributions from small methane sources, which in some cases requires additional analysis of the aerial remote
sensing results. For our analysis of continuous methane emissions distribution curves from the Bridger GML
campaigns (Xia et al., 2024; Kunkel et al., 2023), we restrict our analysis to estimated emission rates >3 kg/hr,
which is the approximate LOD of the Bridger GML remote sensing platform. For MethaneAIR, we use the
275 percentage of area emissions (i.e., diffuse area methane sources) relative to the total methane emissions for the
spatial boundary, which roughly corresponds to all emissions <200 kg/hr (i.e. effectively those emissions below the
point source detection limit of MethaneAIR that flew in multiple campaigns in the US at 40,000ft above ground
level (Chulakadabba et al., 2023)). MethaneAIR characterizes the total regional emissions including the spatial area
emissions at high resolution using a geostatistical inverse modeling framework (Miller et al., 2013) while ingesting
280 high-emitting point source information in the inversion (Chulakadabba et al., 2023; Omara et al., 2024). For
Cusworth et al. (2022) we limit our analysis to the six campaigns where 100% of measured point sources were
attributed to oil/gas sources to avoid non-oil/gas sources being included within their denominator (i.e., total area
methane estimates from TROPOMI inversions). We account for the intermittency of detected methane sources with
 <3 overpasses in Cusworth et al. (2022) by resampling with replacement ($n=1,000$) the source persistence of
285 methane sources with ≥ 3 overpasses for the same campaign, which is consistent with their methodology. We
calculate the percentage contributions of low emitting sources in Cusworth et al. (2022) using Eq. 2: where $\%E_{f<x}$ is
the percentage of total oil/gas methane emissions below an emission rate threshold x (kg/hr), $\%E_{f>10}$ is the
percentage of total emissions contributed from point sources emitting >10 kg/hr, T is the total area emissions



290 measured via TROPOMI inversions (kg/hr), and $P_{<x}$ is the sum of point source emissions below the emission rate
threshold x (kg/hr).

$$\%E_{<x} = (100 - \%E_{>10}) + \left(\frac{P_{<x}}{T} \times 100\right) \quad (2)$$

2.5 Uncertainty calculations

295 Our emission distributions based on facility-level estimates incorporate uncertainty through several steps, such
as the: probabilistic distributions of a select facility being a top 5%, bottom 95% emitter, or facility emitting below
the LOD; emission rate and loss rate distributions produced from facility-level empirical measurements; and flaring
combustion efficiencies. In addition, we incorporate uncertainties from the empirical measurements into our facility-
level model by simulating new empirical emission rates based on the associated method uncertainties. At the
300 beginning of each of the 500 model iterations, we use the reported empirical methane emission rate data and
estimate a new emission rate using a normal distribution with the mean as the initial reported emission rate and the
standard deviation as a percentage of the mean value. These measurement uncertainties are chosen based on the
measurement methodology using the lower percentage uncertainty ranges provided by Fox et al. (2019) for facilities
measured via the OTM-33a ($\pm 25\%$), Gaussian plume dispersion ($\pm 50\%$), and tracer release ($\pm 20\%$) methods. For
305 HiFlow sampler measurements, we use an uncertainty range of $\pm 16\%$ (Riddick et al., 2022), and for chamber-based
measurements, we use $\pm 14\%$ (Williams et al., 2023). Therefore, each model iteration incorporates a unique suite of
empirical measurement data based on the initially reported emissions and their associated uncertainties, which in
turn impacts the probabilistic modeling of the chance of a facility emitting below the method LOD, the empirical
data is used to determine the parameters of the lognormal distributions of loss rates and emission rates, and the
310 ranges of the production bins (SI – Section 1). To calculate the cumulative uncertainty of our facility-level model
estimates, we estimate 500 methane emission distributions and aggregate the 2.5th and 97.5th percentiles of our five
primary facility categories (i.e., low and non-low producing well sites, G&B compressors, T&S compressors, and
processing plants), including VIIRS flare detection emissions, to determine our 95% confidence intervals. This
process is repeated for all simulations at the national-, basin-, and aerial remote sensing boundary levels. For
315 uncertainty calculations in satellite- and aerial-remote sensing studies we use for comparisons, we present the
reported 95% confidence intervals if available.

We calculate the 95% confidence intervals for data from MethaneAIR and Cusworth et al. (2022) using the ratio
of measured point sources to the upper and lower uncertainty bounds of the total area estimates in the calculations of
the percentage contributions of low-emitting methane sources to the total. In cases where multiple aerial campaigns
320 were conducted in the same oil/gas basin by the same study, we average the percentage contributions for all surveys
including the upper and lower uncertainty bounds. For Cusworth et al. (2022), we do not use the reported
uncertainty intervals of their point source detections in our uncertainty calculations since we employ various
emission rate thresholds in our comparisons without a clear understanding of how the point source uncertainties

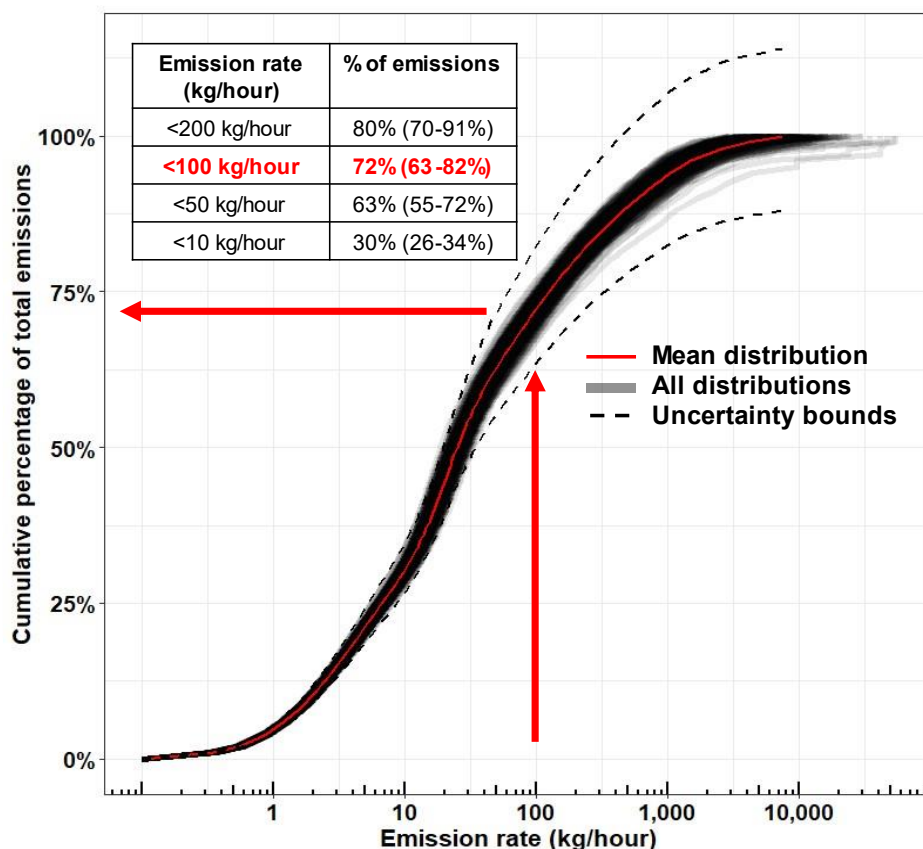


would change depending on the different thresholds, meaning that our uncertainty bounds for the Cusworth et al.
325 (2022) results may be conservative.

3 Results

3.1 Distribution of emission rates at the national scale 330

Based on the results from our facility-level model simulations, we estimate that 72% (95% confidence interval: 63-82%) of total methane emissions from the upstream/midstream sector in the CONUS for 2021 originate from facilities emitting methane at rates <100 kg/hr (Fig. 3). For other emission rate thresholds, we find that 30% (26-34%) of total emissions come from facilities emitting <10 kg/hr, which corresponds to the lower thresholds of
335 aircraft-based aerial remote sensing studies (Kunkel et al., 2023; Thorpe et al., 2024; Johnson et al., 2021; Xia et al., 2024; Cusworth et al., 2022), and 80% (70-91%) of total emissions come from facilities emitting <200 kg/hr. This result suggests that a large majority of oil/gas emissions in the CONUS are not detectable by existing satellite remote-sensing point source imagers (Sherwin et al., 2023). We find that the emission rate threshold corresponding to 50% of cumulative methane emissions from upstream/midstream facilities in the CONUS for 2021 is 25 (19-33)
340 kg/hr.



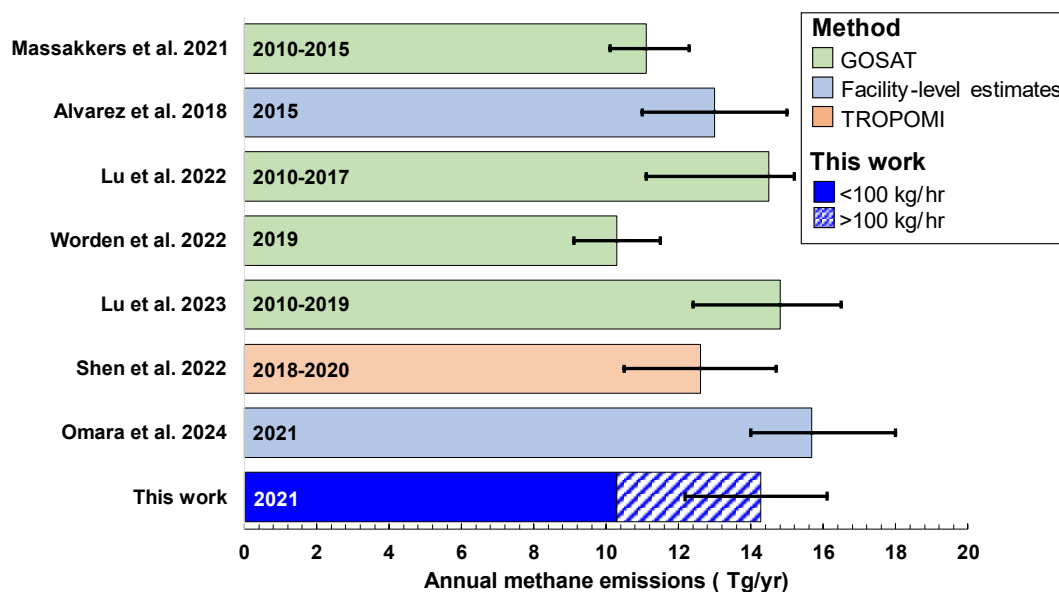
345 **Figure 3:** Results from 500 estimated facility-level emission distributions showing the cumulative percentages of total methane emissions contributed from facilities emitting below methane emission rate thresholds. For example, facilities emitting <100 kg/hr account for 72% (63-82%) of total methane emissions. The inset table in the upper left displays the total percentage of methane emissions contributed from discrete emission rate thresholds with 95% confidence intervals.

350 The distribution for our national-level methane emissions follows an S-shaped curve, noting that the x-axis (i.e., facility-level methane emission rates) is presented in the log₁₀ scale. From 0.1 to 1 kg/hr, we observe a plateau in the distribution curve indicating that increasing emission rates within this range do not significantly increase the percentage contribution to total regional emissions (Fig. 3), similar to the findings in Ravikumar et al. (2019) From 1 to 100 kg/hr, we see a sharper rise in the emission distribution, indicating that increasing emission rates at this range lead to a more substantial contribution to total methane emissions, and account for 68% (60 – 75%) of total methane emissions (Fig. 3, Table S4). Above an emission rate threshold of 100 kg/hr, we see an exponential decline in the percentage contributions of total emission with increasing emission rates, with total methane emissions in this range amounting to 28% (18 – 37%) of the total oil/gas emissions. Facilities emitting at the 1-10 kg/hr and 100-1,000 kg/hr



ranges contribute a similar cumulative percentage at 26% (23 - 29%) and 22% (18 - 26%) respectively. Similar
percentage contributions are also observed between the 0.1-1 kg/hr and >1,000 kg/hr ranges at 4.5% (4.0 - 5.1%) and
360 6.1% (2.6 - 13%) respectively. Overall, we find that the highest contribution to total national CONUS methane
emissions occurs from facilities emitting in the 10-100 kg/hr range at 42% (37 - 46%). In terms of facility counts,
from the 673,940 total active oil/gas facilities we estimate in the CONUS for 2021, we estimate that essentially all
(i.e., ~99.9%) of these facilities emit methane below 100 kg/hr.

Our facility-level model estimates total methane emissions from US upstream/midstream oil/gas emissions
365 for 2021 to be 14.3 (12.6 - 16.3) Tg/yr, or 1,634,000 (1,438,000 - 1,857,000) kg/hr (Fig. 4), which corresponds to a
gross gas production normalized loss rate of 2.4%, assuming a uniform 80% methane content in natural gas across
oil/gas producing regions in the CONUS. This national emission total of 14.3 Tg/yr is more than double the EPA
Greenhouse Gas Inventory Report for natural gas and petroleum systems in 2021, excluding post-meter and
distribution methane emissions (Inventory of U.S. Greenhouse Gas Emissions and Sinks, 2024). We compare our
370 total national estimates to those made by seven studies that predominantly utilize satellite-based remote-sensing
platforms such as GOSAT and TROPOMI inversions (Lu et al., 2022, 2023; Shen et al., 2022; Maasackers et al.,
2021; Worden et al., 2022) except for Alvarez et al. (2018) and Omara et al. (2024) who developed unique facility-
based modeling approaches using empirical measurement data collected from multiple oil/gas basins in the CONUS
(Fig. 4). Our estimate of national methane emissions overlaps with six out of seven other national estimates of
375 oil/gas methane emissions for the US, with a combined average of 13.1 (ranging from 11.1 - 15.7) Tg/yr. We do not
estimate methane emissions from gathering/transmission/distribution pipelines, post-meter emissions, abandoned oil
and gas wells, and refineries due to the scarcity of measurement-based data for these sources. Total methane
emissions from these sources emit ~2 Tg/year of methane emissions based on other studies (Williams et al., 2021;
Alvarez et al., 2018; Omara et al., 2024; Weller et al., 2020; Inventory of U.S. Greenhouse Gas Emissions and
380 Sinks, 2024). Overall, our total national estimate of CONUS methane emissions for 2021 shows good agreement
with multiple independent and recent measurement-based estimates.



385 **Figure 4:** Comparison of total CONUS oil/gas emissions for 2021 from this facility-level measurement-based
 inventory compared to empirical estimates from other studies. Bars are colored according to the methodology used
 to derive the total national estimates, and the years within the bars represent the corresponding time periods for the
 estimates. Our total estimates for “This work” do not include emissions from other oil/gas methane sources such as
 abandoned oil and gas wells, transmission/gathering/distribution pipelines, post-meter emissions, and refineries.
 390 Emission estimates from Omara et al. (2024) do not include methane emissions from abandoned oil and gas wells.
 We assume that the remote sensing estimates (i.e., GOSAT and TROPOMI) include all oil/gas methane sources,
 including downstream emissions.

3.2 Distribution of emission rates at the basin-level scale

395 Among the top twelve emitting oil/gas basins in the CONUS, we observe variations among the different
 basins in terms of the methane emission distributions, especially at higher emission rate thresholds (Fig. 5). The
 majority of the top twelve emitting oil/gas basins in Fig. 5 show higher percentage contributions from facilities
 emitting <100 kg/hr when compared to our national estimate of 72% (63 – 82%) (Fig. 3). These percentage
 contributions vary from ~80% in the Permian, Appalachian, and Eagle Ford basins, up to ~90% in the oil-dominant
 400 San Joaquin basin. Only the Anadarko and Denver basins have notably lower contributions to total emissions at the
 100 kg/hr threshold at ~65% compared to the national level, which is still a significant majority of total methane
 emissions. Despite these variations, our facility-level model estimates that the majority of total national oil/gas
 emissions are consistently contributed from facilities emitting <100 kg/hr for the top 12 emitting basins.

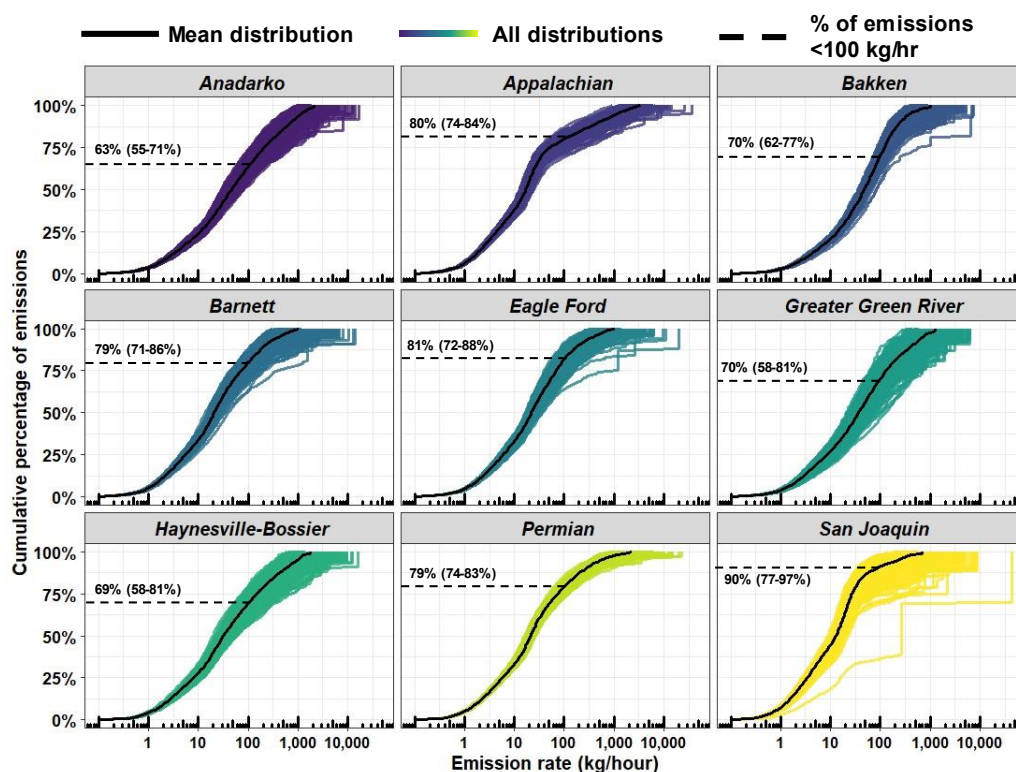
405 Our modeled facility-level emission distributions for the top 12 emitting oil/gas basins all follow an S-
 shaped curve (Fig. 5) like the national distribution (Fig. 3), albeit with certain variations. For all basins, the initial



plateau in the emissions distribution curves ends at around 1 kg/hr before beginning to rise more steeply. For the Appalachian and San Joaquin basins, the second plateau is at the 20-50 kg/hr emission rate threshold (Fig. 5). For the remaining basins, the rise in the emission distribution curves plateaus gradually, indicating a more consistent relationship of emission rate thresholds to their contribution to total emissions. The variability displayed among the 500 basin-level simulations differs among the oil/gas basins, with less spread in the 500 estimated methane emissions distributions for the Appalachian, Anadarko, and Permian basins compared to the Uinta, Denver-Julesburg, and San Joaquin basins (Fig. 5). These variations are likely caused in part by the overall total basin-level methane emissions, where an extremely high estimated methane emission rate would have a greater impact on the percentage contribution to the total for basins with lower overall emissions (e.g., the apparent outlier distributions present in the San Joaquin basin in Fig. 5). We discuss below other plausible causes for basin-to-basin variability in the estimated methane emission distributions.

In terms of total methane emissions, the top two emitting oil/gas basins are the Permian and Appalachian, which collectively account for 5.3 (4.1 – 7.2) Tg/year (Fig. S1) or 37% of total upstream and midstream oil/gas methane emissions. This exceeds the cumulative contribution from the other seven highest emitting oil/gas basins which collectively account for 3.4 (2.5 – 6.1) Tg/yr. Notably, we find that the highest emissions in the CONUS occur from regions outside of any basin boundary 3.9 (3.3 – 5.1) Tg/year. Our estimates for basin-level total emissions also show good agreement with remote-sensing satellite-based observations (Fig. S1), except for the Appalachian, Bakken, Greater Green River, and Denver-Julesburg basins where our results are consistently more than double those from the remote-sensing studies that used a prior-emission based inversion result (Shen et al., 2022; Lu et al., 2023). These four basins are located in regions with relatively low TROPOMI observation counts and densities compared to other regions in the CONUS (Shen et al., 2022), in addition to other factors that could influence satellite-based inversions such as the presence of many non-oil/gas sources such as coal, livestock, and landfills. Overall, our estimates of total basin-level emissions are consistent with satellite-based observations.

430



435 **Figure 5:** A) Results from 500 model simulations showing the cumulative methane emissions distribution curves for total upstream/midstream oil/gas methane emissions for the top nine emitting oil/gas basins in the CONUS for 2021. The model averages for each basin are shown in solid black lines. Inset dashed lines represent the percentage contributions of total emission from sources emitting <100 kg/hr. Emission distribution curves for the remaining eleven oil/gas basins in the CONUS are shown in Fig. S15, and a map of the spatial boundaries used for the different oil/gas basins is shown in Fig. S16.

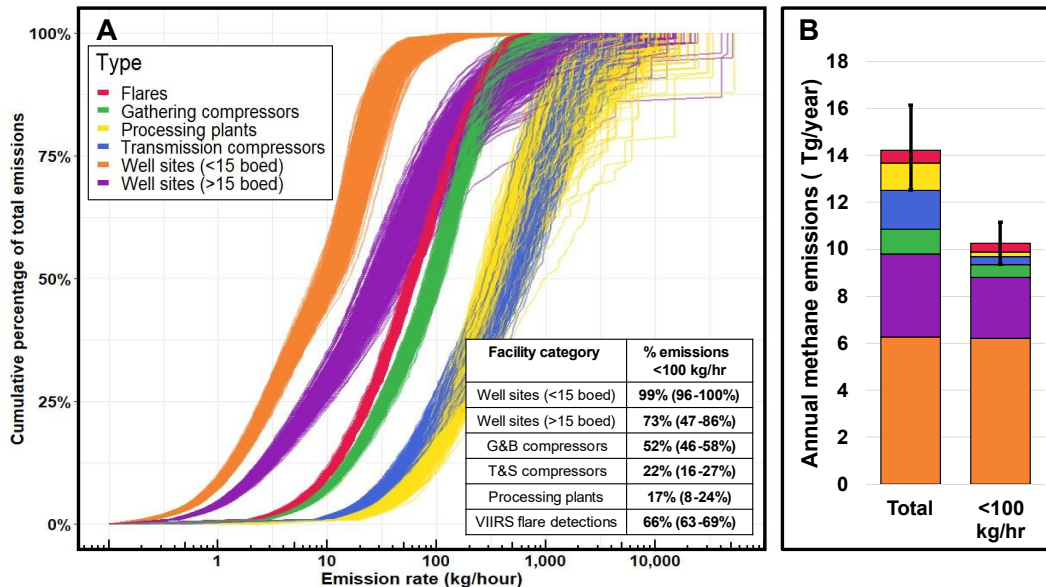
440 3.3 Distribution of emission rates by facility category

445 We find significant variations in the methane emission rate distribution curves among the different facility categories (Fig. 6A). Over 50% of total methane emissions from low and non-low production well sites, flares, and G&B compressor stations occur from facilities emitting <100 kg/hr (Fig. 6A). In contrast, only 17% (8-24%) of emissions from processing plants and 22% (16-27%) of emissions from T&S compressor stations are contributed from facilities emitting <100 kg/hr. Similar variability is also observed at other emission rate thresholds, such as only 1% (0-2%) of total emissions for T&S compressor stations and processing plants originating from facilities emitting at rates <10 kg/hr, compared to 50% (43-58%) from low producing well sites and 30% (24-35%) from non-low producing well sites (Fig. 6A). At higher emission rate thresholds, we find that 33% (20-45%) of total emissions from T&S compressors and processing plants are emitted from facilities <200 kg/hr, compared to 84% (68-93%)



450 from non-low producing well sites (>15 boed), 86% (83-88%) from VIIRS flare detections, 78% (70-86%) from G&B compressor stations, and essentially 100% of emissions from low producing well sites.

A breakdown of the 673,940 total facilities in our model has 541,970 as low-producing well sites, followed by 121,824 non-low-production well sites, 4,181 G&B compressor stations, 2,033 T&S compressor stations, 919 processing plants, and 3,153 VIIRS flare detections. Overall, we estimate that roughly 70% of total CONUS oil/gas methane emissions for 2021 come from production well sites, of which 44% are from low-production well sites with combined oil/gas production <15 boed, and the remaining 26% from non-low production well sites (>15 boed) (Fig. 6B). 26% of total methane emissions are from midstream facilities, with 11% from T&S compressors, 8% from processing plants, 7% from G&B compressor stations, and the remaining 4% from VIIRS flare detections. Based on the population counts for each facility category and their corresponding total methane emissions, the average methane emission rate per facility category is highest for processing plants at 145 (109 – 277) kg/hr, followed by 92 (72 – 118) kg/hr for T&S compressor stations, 28 (26 - 32) kg/hr for G&B compressor stations, 3.3 (2.8 – 4.9) kg/hr for non-low producing well sites, and 1.3 (1.1 – 1.5) kg/hr for low producing well sites.



465 **Figure 6:** A) Results from an ensemble of 500 estimated methane emission distributions showing the percentage of total methane emissions among facility categories contributed from facilities emitting at rates below an emission rate threshold. The inset table on the bottom right displays the discrete percentage contributions to total methane emissions contributed from facilities emitting <100 kg/hr. B) Breakdown of total annual methane emissions contributed from all emitting facility categories and those emitting at rates <100 kg/hr.

470 *Only single percentiles are used for the y-axis in A) due to the large volume of data (i.e., ~2 million data points) available for the figure. The use of single percentiles causes instances of duplicated emission rates for ascending percentiles at upper emission rate thresholds for different facility categories, leading to the appearance of segmented methane emissions distribution curves for some facility categories.



**Note that the emission distributions for flares represent VIIRS flare detections which could include multiple

475 3.4 Comparisons to aerial remote sensing studies

We perform comparisons of the percentage contributions of methane emissions from facilities emitting below discrete emission rate thresholds between seven aerial remote sensing campaigns across four distinct regions and our estimated facility-level results (Fig. 7). The aerial remote sensing technologies include data from Bridger
480 GML measurements (Kunkel et al., 2023; Xia et al., 2024), MethaneAIR (Omara et al. 2024; Miller et al. 2023), and the results from Global Airborne Observatory and next-generation Airborne Visible/Infrared Imaging Spectrometer campaigns (Cusworth et al., 2022) which are also included in the aerial detections used by Sherwin et al. (2024).

In a comparison of the percentage contributions to total emissions from low-emitting sources between our facility-level model estimates and the aerial remote sensing campaigns presented in Fig. 7, we find that point source
485 contributions are comparable across the aerial remote sensing campaigns. Our comparisons to the available flight results from MethaneAIR, which quantifies both total regional methane emissions and high-emitting point sources >200 kg/hr from the same aerial platform (Chulakadabba et al., 2023), show close agreement between our facility-level estimates and the only available MethaneAIR campaigns in the Uinta and Permian basins for facilities emitting <200 kg/hr (Fig. 7A). For the MethaneAIR flight in the Uinta basin, we estimate that 92% (58 - 100%) of total
490 oil/gas methane emissions are from sources emitting <200 kg/hr compared to 88% (85 - 92%) from MethaneAIR (Fig. 7A). For the two available flights in the Permian basin from MethaneAIR, we estimate total contributions from <200 kg/hr sources at 82% (63 - 93%) compared to the 72% estimated by MethaneAIR (Fig. 7A).

For the multiple aerial remote sensing campaigns performed by Cusworth et al. (2022), our estimates statistically overlap for discrete emissions rate thresholds of <200 kg/hr and <100 kg/hr (Fig. 7A, Fig. 7B). For the
495 Bridger GML remote sensing campaigns (Xia et al., 2024; Kunkel et al., 2023), we find good agreement in the percentage of total emissions contributed from facilities emitting <200 kg/hr and <100 kg/hr compared to our facility-level model estimates (Fig. 7A, Fig. 7B). A comparison of continuous emissions distribution curves between our facility-level emission distributions and two Bridger GML aerial remote sensing campaigns (Xia et al., 2024; Kunkel et al., 2023) targeting four oil/gas basins is shown in Fig. S14. The Bridger GML aerial sampling platform
500 has the lowest LOD among the aerial campaigns we analyze in this work and a similar source resolution (i.e., 30 meters) to our facility-level model (i.e., 50 meters), allowing for a more detailed comparison of continuous emission distribution curves due to the higher number of detected methane sources at low emission rates provided by Bridger GML surveys. We see close agreement between our facility-level methane emission distribution curves and the observed emissions by Bridger GML in the four-basin aggregate provided by Xia et al. (2024) (Fig. S14A) and the
505 Permian remote sampling campaign (Fig. S14B) by Kunkel et al. (2023), with the measured emissions from the Bridger GML surveys overlapping with our facility-level model simulations throughout the continuous distribution



of methane emission rates. Overall, our findings show that our facility-level estimates closely agree with the results from multiple aerial remote sensing campaigns from different regions and using various measurement methods.

510

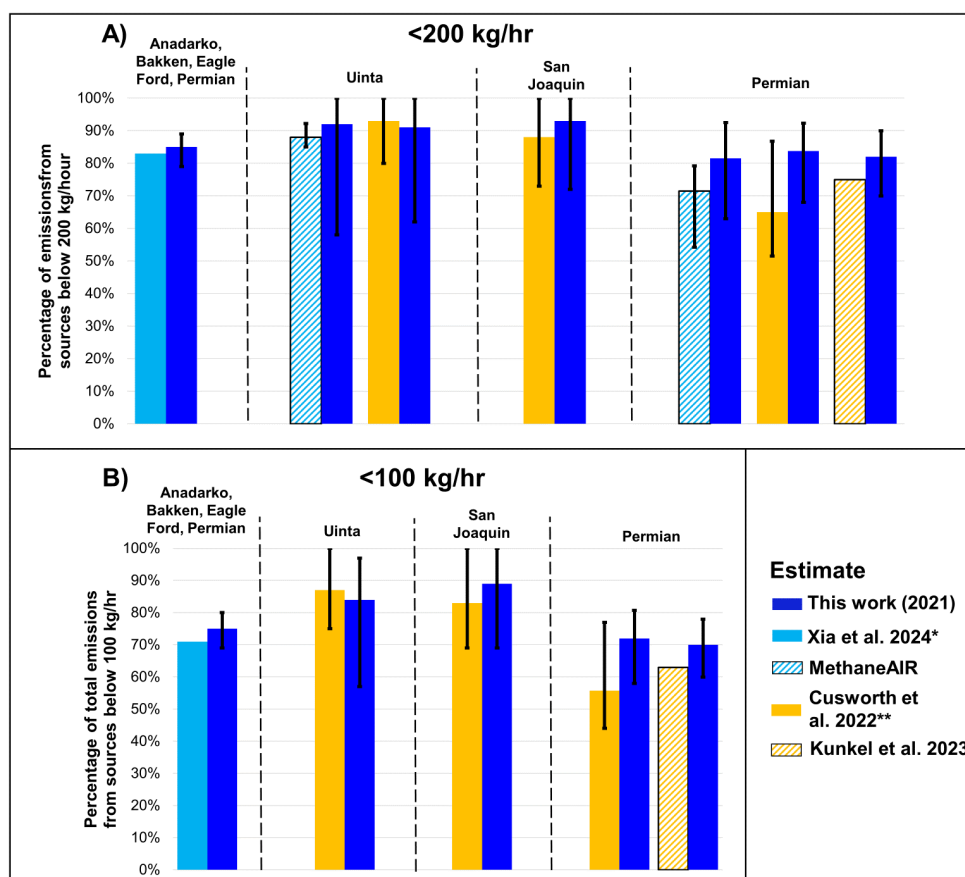


Figure 7: Comparisons of the cumulative percentage of oil/gas methane emissions from all oil/gas facilities emitting <200 kg/hr (A) and <100 kg/hr (B) between our facility-level empirical emissions estimates and aerial remote sensing campaigns. Bars are colored according to the study and grouped according to the target oil/gas basin(s). All results from the facility-level simulations (i.e., this work) are constrained to the spatial boundaries of the aerial campaigns for direct comparisons (note that for a given basin, spatial boundaries might be slightly different). Uncertainty bars for the facility-level simulations are the 2.5th and 97.5th percentiles of 500 simulations. Maps of all spatial boundaries used for comparisons are provided in Fig. S2.

515



520 *The surveyed oil/gas basins in Xia et al. (2024) are the Anadarko, Bakken, Eagle Ford, and Permian basins. The exact surveyed boundaries are
not available from Xia et al. (2024), therefore the comparisons between this work are for the entire four oil/gas basins.

**Results presented by Cusworth et al. (2022) in the Permian oil/gas basin are the average of four Permian aerial remote sensing campaigns.

525 **4 Discussion**

Understanding how facilities with different magnitudes of emissions contribute to total regional emissions
has direct policy implications for methane quantification and mitigation, such as the selection of
measurement/screening methods with the appropriate detection sensitivities (Ravikumar et al., 2018). We find that
530 roughly three-quarters of total oil/gas methane emissions from the upstream/midstream sectors come from facilities
emitting at rates <100 kg/hr, which is the threshold used to define a “super-emitting” oil/gas source by the EPA
(EPA’s Final Rule for Oil and Natural Gas Operations Will Sharply Reduce Methane and Other Harmful Pollution.,
2024). While mitigating emissions from sites emitting above this threshold is important, our results also show the
essentiality of expanding beyond solely on super-emitter mitigation - as the cumulative contribution of lower-
535 emitting sites accounts for a large majority of emissions across US oil/gas basins. Facility-level, measurement-based
data collected in some other countries present a similar story. From a sample of sites measured via Bridger GML
remote sensing platform in British Columbia, Canada (Tyner and Johnson, 2021), roughly 60% of the total
quantified oil/gas site-level emissions originate from sites emitting <32 kg/hr. In Romania, a site-level
measurement-based inventory (Stavropoulou et al., 2023) find that oil production facilities emitting <100 kg/hr
540 contribute 78% of total oil/gas methane emissions in the studied region. In short, the high percentage contribution
from lower-emitting (<100 kg/hr) oil/gas facilities that account for a large majority of total emissions is not unique
to the US and is likely present in other countries as well. A combination of approaches that characterize entire
emission distributions across populations of sites (i.e., not just focusing on measuring super-emitters) and
quantification of regional-level emissions is needed in other countries to quantify the relative contributions of low-
545 emitting sources that in aggregate can be significant sources of overall oil/gas methane emissions.

While most of the focus in this work centers around quantifying the percentage contributions of oil/gas
methane sources emitting below one discrete emission rate threshold (i.e., <100 kg/hr, per EPA’s definition of a
super-emitter) our assessment illustrates the importance of a complete characterization of emissions which gains
importance as newer methane monitoring technologies have different LODs. For example, the effective LOD at high
550 probabilities of detection for available point source imaging satellites of ~200 kg/hr (Jacob et al., 2022) would only
be able to quantify 20% (9-30%) of all oil/gas point sources in the CONUS, if the full oil/gas sector was mapped in
its entirety, based on our facility-level results.

Point source-focused remote sensing platforms offer the advantage of rapidly surveying large areas (i.e.,
100’s-1,000’s km²) which facilitates the detection and quantification of the small number of high emitting point



555 sources, which is a finding repeated in multiple studies (Cusworth et al., 2022; Brandt et al., 2016; Duren et al.,
2019; Sherwin et al., 2024). In contrast, logistical constraints often limit the sample sizes for ground-based vehicle
sampling platforms, however, these limitations can be overcome with stratified random, representative sampling and
statistical analysis approaches like this work. Ground-based measurement platforms provide much lower LODs (i.e.,
<1 kg/hr) when compared to remote sensing platforms, which are necessary to quantify emissions from the large
560 number of small methane sources we find that contribute roughly three-quarters of total regional oil/gas emissions in
the CONUS, and will only improve as additional ground-based measurements are gathered. Overall, our main
findings highlight the importance of methods that can rapidly locate the small number of high-emitting point sources
we estimate, but our findings emphasize the need to account for the disproportionately large majority percentage of
total regional oil/gas emissions that are emitted from smaller diffuse methane sources.

565 When extrapolating our facility-level model results to the basin-level we see variations among the emission
distribution curves for different oil/gas basins, but still find that most methane emissions come from facilities
emitting <100 kg/hr. The variations in the emission distribution curves for different basins are driven by many
factors, such as the: production characteristics, number and density of facilities, different types and relative counts of
facility categories, the availability of empirical measurement data used to model emissions, and the total oil/gas
570 methane emissions (i.e., the denominator). For example, the Appalachian basin is dominated by a high number of
older low-production well sites (Deighton et al., 2020; Riddick et al., 2019; Enverus, 2024) with fewer midstream
facilities such as processing plants and G&B compressors, which contrasts with the Bakken basin where we find a
high number of midstream facilities, high-producing well sites, and VIIRS flare detections (Elvidge et al., 2016;
Enverus, 2024). When comparing the emissions distribution curves for the Bakken and Appalachian basins (Fig. 5),
575 we observe higher contributions from lower-emitting facilities for the Appalachian compared to the Bakken. An
example of differences in basin-level production is shown in Fig. S9 and Fig. S10, where we see variable profiles
among the different oil and gas-producing basins in terms of well site production characteristics, which are the main
source of total methane emissions in this work (Fig. 6). We also observe the influence of total basin-level emissions
on the variability among our emission distribution curves, where large emitting sources in the San Joaquin basin can
580 lead to high variability among the estimated emission distribution curves compared to the Permian basin which has
roughly ten times the total emissions compared to the San Joaquin (Fig. 5). We note that a direct comparison of our
model results with aerial remote sensing methods may be limited, in part, by methodological differences in methane
quantification approaches (and underlying uncertainties). The remote sensing observations assessed here as
snapshots may capture facility-level emission distributions that are not well represented in annually averaged
585 methane emissions distributions, as we estimate here. Nevertheless, we find broad agreement with these independent
aerial remote sensing estimates at the basin scale and across smaller spatial domains, as discussed. Ultimately, as
many characteristics will influence methane emissions distribution curves among different oil/gas producing regions
in the CONUS, mitigation strategies will need to be structured accordingly to the region they are targeting.

590 Our results find that over half of cumulative methane emissions from three different facility categories
come from facilities emitting <100 kg/hr, including methane emissions from VIIRS flare detections. We show how



the large contributions from small methane sources to total regional emissions are not unique to any one facility category, but it is important to contextualize our emission distribution curves with the corresponding total regional emissions. Our facility-level estimates find that the main source of oil/gas methane emissions in the CONUS are oil/gas production well sites, of which the low production category is responsible for 44% (39 – 49%) of the total
595 estimated oil/gas methane emissions in the CONUS in 2021. Low-producing well sites, also known as “marginal wells”, have been shown in previous work to be a significant source of methane emissions, especially relative to their contribution to overall oil/gas production (Omara et al., 2022; Deighton et al., 2020). Omara et al. (2022) found that marginal wells contributed anywhere from 37%-75% of total methane emissions from production well sites, which is similar to our estimates (i.e., 64%). Despite low production well sites having a lower mean emission rate
600 compared to other facility categories, the large facility counts result in significant aggregate total emissions of methane. This implies that detection and mitigation strategies to reduce methane emissions from these and other low-emitting oil and gas infrastructure (e.g., abandoned oil/gas wells) would require alternative mitigation and detection approaches compared to those for the small number of super-emitting emission sources. For detection, measurement methods that can measure emission rates between 0.1-100 kg/hr are required, since this range makes
605 up 72% of total methane emissions (Fig. 3) as modeled herein. In terms of methane mitigation policy, financial incentives, like the USD 4.7 billion from the Biden Bipartisan Infrastructure Law for abandoned wells, could be used to prioritize the repair of old and leak-prone production well sites, as these low-producing well sites only account for a small fraction (i.e., 5.6% in 2019) of total oil/gas production (Omara et al., 2022).

Although the empirical data used in our analysis includes a smaller sample of super-emitting facilities
610 relative to those captured by remote sensing platforms (Sherwin et al., 2024; Duren et al., 2019), our use of production-normalized loss rates and lognormal distributions to estimate facility-level methane emission rates anticipates and accounts for the possibility of finding low-probability, high-magnitude emissions that occur at rates beyond those that appear in our dataset of empirical observations. Our highest empirical emission rate is 1,360 kg/hr for a T&S compressor station, whereas our maximum estimated facility-level emission rate across all 500 facility-
615 level emission distribution curves averages 7,500 kg/hr (3,000 - 21,000 kg/hr).

We see good agreement between our facility-level model results and a majority of aerial remote sensing studies, which are expected to capture a wide range of high-emitting facilities in a survey region. For example, when comparing our model results to Kunkel et al. (2023) and Xia et al. (2024) we find that our estimated methane emissions closely match the distribution of methane emissions measured in Bridger GML surveys (Fig. S14). In the
620 same analysis, we estimate nearly identical total emissions from facilities emitting >100 kg/hr when compared to the results of Kunkel et al. (2023). We also find good agreement to satellite remote sensing estimates of emissions, such as our basin-level (Fig. S1) and national-level comparison to satellite inversions (Fig. 3), and other aerial remote sensing study regions (Table S2). Our comparisons of the contributions of low-emitting sources below discrete emission rate thresholds also agree closely with recent MethaneAIR, Kairos Aerospace, GAO, and AVIRIS-NG
625 aerial surveys, whose results also highlight the importance of small methane sources to overall oil/gas methane emissions. This broad agreement across multiple studies differs from those of Sherwin et al. (2024) who suggest



majority of total emissions from a small fraction of high-emitting sites. Notably, many of the same aerial measurements that are used in Sherwin et al. (2024) are used for comparisons in this work (i.e., Cusworth et al. (2022)) (Fig. 7) that appear to indicate that the estimation of the overall methane emissions from small-emitting sources in Sherwin et al. (2024), in particular those below aerial detection limits used in their study, may be an underestimate.

The percentage contribution of facilities emitting below an emission rate threshold is a ratio where the numerator is the sum of the total point source emissions (i.e., emissions above an emission rate threshold) and the denominator is the total regional oil/gas emissions. Our comparisons of the percentage contributions of point sources to regional emissions for various aerial remote sensing studies and our facility-level estimates agree. It is worth noting that our calculations of the point source percentage contributions from the aerial remote sensing studies assume that the regional estimate (i.e., the denominator) is entirely from oil/gas sources, which may be reasonable for the Permian basin but is likely not the case for the San Joaquin basin which contains multiple significant non-oil/gas methane sources (Duren et al., 2019). MethaneAIR provides a novel remote sensing approach where high-emitting point sources, distributed area sources and total regional emissions are quantified using the same aerial platform, providing the ability to directly measure high-emitting point source and diffuse area contributions to total regional estimates. In the work by Xia et al. (2024) they combine measurements from Bridger GML across four oil/gas basins and use component-level simulations to account for facilities emitting below the 3 kg/hr LOD of Bridger GML. Other approaches also exist, such as Cusworth et al. (2022) who use TROPOMI inversions as the denominator, with their numerator obtained from the point source emissions quantified from their aerial detection platforms above a certain threshold. Similarly, Sherwin et al. (2024) present point source emission rates from several aerial campaigns as their numerator, with the denominator calculated from a combination of a component-level bottom-up model for production well sites (Rutherford et al., 2021) and emission estimates for midstream facilities emitting below aerial detection limits using emission factors from the 2023 GHGI (Inventory of U.S. Greenhouse Gas Emissions and Sinks, 2024). These remote sensing studies largely rely on aerial detections of generally higher-emitting point sources as part of their numerator, which has variable LODs depending on the target region, topography, measurement technology, presence of co-located non-oil/gas methane sources (i.e., source attribution), weather conditions, infrastructure density, and infrastructure type(s). These variables pose additional challenges when quantifying the contributions from facilities emitting above/below specific emission rate thresholds, which are critical information to inform mitigation policy. Assessing performance, tracking mitigation, and accurate reporting requires building a comprehensive picture of emissions by characterizing all emitters big and small, and reconciling with total basin/sub-basin level emissions. Ultimately, the key seems to be merging the best data from both approaches to build a hybrid inventory, ideally using a multi-tiered system with multiple methods that span a range of LODs that allow for gathering empirical measurements from facilities emitting at all parts of the methane emission distribution curve. Our study is a step in that direction considering measurement-based data while also presenting a robust comparison with available independent remote sensing measurements. At the same time, large-area aggregate emissions data obtained from wide-area remote sensing mapping or mass balance surveys can better constrain total regional emissions (e.g. Cusworth et al. 2022; Omara et al. 2024) towards a more empirically robust



665 denominator in characterizing the relative contributions of small emission and high emission sources to total emissions.

We show that our facility-level emission models produce national- and basin-level methane emissions estimates that are in good agreement with other independent measurement-based studies. However, we note the following limitations/biases that could be improved with future data collection efforts. The empirical measurements that we use in our model are representative of the year and time they were measured (i.e., 2010-2020), meaning that they would not reflect any updates in regulatory practices or changes in facility operational and emission management practices. Furthermore, there are several oil/gas methane emission sources that we do not account for in our estimates, which include: gathering/transmission/distribution pipelines, oil refining and transportation, abandoned oil/gas wells, offshore oil/gas infrastructure, post-meter sources, and oil/gas distribution infrastructure in urban areas. For some sources omitted in this work such as abandoned oil/gas wells, their inclusion would likely lead to a higher contribution from low-emitting facilities, since the highest recorded emission rate from an abandoned oil/gas well is 76 kg/hr (Riddick et al., 2024). For others such as oil refineries, their inclusion would likely lead to a lower contribution from small methane sources given their low facility counts and high per-site emissions (Duren et al., 2019). Despite their omissions, total methane emissions from these sources are currently estimated to account for 5-10% (Alvarez et al., 2018; Williams et al., 2021; Inventory of U.S. Greenhouse Gas Emissions and Sinks, 2024; Riddick et al., 2024) of total oil/gas sectoral emissions. Our estimates also utilize empirically measured emission rates from ground-based sampling platforms which are limited in number, especially in the case of processing plants (n=20) and T&S compressor stations (n=50) (Table S1). Finally, we include a small number (i.e., 5% of total empirical data used in the model) of measurements gathered using ground-based component/source-level sampling methods from two studies (Deighton et al., 2020; Riddick et al., 2019). All measurements from these two studies targeted the lowest production cohort of production well sites and exhibited statistically lower emission rates than those gathered using facility-level ground-based methods (Figure S4) for the same well site production cohort, meaning that any bias introduced by the inclusion of these measurements would lead towards the underestimation of total emissions and/or the percentage contributions from low-emitting sources. Despite these limitations, we have shown that our results are broadly in agreement with satellite- and aerial-based remote sensing studies at national/basin/local scales, and other facility-level estimates.

Going forward, several approaches can be used to better understand the percentage contributions from facilities emitting at different leak rate thresholds, and ultimately improve our understanding of oil/gas methane emissions in the CONUS and around the world. A combination of multiple satellite and aerial remote sensing approaches and synthesis of their data by bringing in point source detections at multiple thresholds at the same time characterizing total regional emissions as demonstrated using a compilation of multi-scale measurements seems a viable pathway towards building a more complete picture of the overall methane emissions. Combining aerial and satellite remote sensing measurements with ground-based site/facility-level estimates presents itself as an effective next step, as implemented/suggested by prior studies (Alvarez et al., 2018; Allen, 2014). Aerial or satellite remote sensing platforms focused on point source detection offer the ability to rapidly locate the small number of the highest



700 emitting facilities that contribute a disproportionate fraction of emissions, offering valuable data on specific facility
locations that allow for rapid mitigation. However, more direct observational approaches are needed to acquire total
emissions data which according to this study is dominated by small-emitting sources that are undetected by high-
emitting point source detection systems. Facility-level population-based approaches can account for the lower-
emitting facilities that contribute the most total oil/gas methane emissions, which is needed for accurate emission
705 reporting and understanding the contributions of total emissions above/below emission rate thresholds. The ground-
based estimates can be further constrained by large-area aggregated emission quantification provided by regional
remote sensing or mass balance mapping approaches (Shen et al., 2022; Omara et al., 2024; Jacob et al., 2022)
towards producing a more robust overall emission quantification.

5 Conclusions

710 In conclusion, our work highlights several key aspects of oil/gas methane emission rate distribution curves
in the CONUS for 2021, which include:

1. A large majority (72%) of total national continental oil/gas methane emissions in the US originate from
low-emitting facilities (<100 kg/hr).
2. Emission rate distributions vary among different oil/gas basins, but among the top nine producing basins
715 we consistently find that most methane emissions (63%-90%) originate from oil/gas facilities emitting at
rates <100 kg/hr.
3. We estimate that production well sites emit 70% of total oil/gas methane emissions in the CONUS, with
44% contributed from low-producing well sites (<15 boed) which is nearly half of total national US oil/gas
methane emissions.
- 720 4. Our results are in broad agreement with those from independent aerial/satellite remote sensing estimates,
both in comparing contributions from discrete emission rate thresholds and continuous emissions
distribution curves, which emphasize the importance of small diffuse methane sources to total oil/gas
methane emissions.

Our results highlight, and quantify, the significant contributions of the large number of low-emitting oil/gas
725 facilities to total regional/basin/local oil/gas methane emissions in the CONUS for 2021. In addition to the CONUS,
the small oil/gas methane sources are likely a significant component of total regional emissions in other countries as
well as recent data suggest from Romania and Canada (Stavropoulou et al., 2023; Tyner and Johnson, 2021) and
would need to be further investigated to build a comprehensive assessment of small-emitting methane emissions and
their relative contributions to total oil/gas methane emissions globally. This work emphasizes the need for multi-
730 scale approaches to quantify total regional oil/gas methane emissions; and at the same time characterize and account
for the large contribution from small emission sources dispersed across a wide area, in addition to incorporating data
on high-emitting point sources towards producing overall robust methane emission quantification.



Data availability

735 All estimated methane emission rate distributions at the national, basin, or small target scale are available upon request. Empirical measurement data used in the estimation of the methane emission distribution curves is available from the references listed in Table S1.

Code availability

R code used to create the methane emission distribution curves and figures is available upon reasonable request.

740

Author contributions

JPW and RG designed this study. JPW created the code used to produce all results, with inputs from MO, KM, DZA, and AH. MethaneAIR analysis was provided by JB, MS, and SW. Multi-sensor airborne intercomparison was performed by JPW and RG. JPW prepared the manuscript with input from all co-authors.

745

Competing interests

The authors declare that they have no conflict of interest.

750

References

755 Allen, D. T.: Methane emissions from natural gas production and use: reconciling bottom-up and top-down measurements, *Current Opinion in Chemical Engineering*, 5, 78–83, <https://doi.org/10.1016/j.coche.2014.05.004>, 2014.

Alvarez, R. A., Zavala-Araiza, D., Lyon, D. R., Allen, D. T., Barkley, Z. R., Brandt, A. R., Davis, K. J., Herndon, S. C., Jacob, D. J., Karion, A., Kort, E. A., Lamb, B. K., Lauvaux, T., Maasakkers, J. D., Marchese, A. J., Omara, M., Pacala, S. W., Peischl, J., Robinson, A. L., Shepson, P. B., Sweeney, C., Townsend-Small, A., Wofsy, S. C., and Hamburg, S. P.: Assessment of methane emissions from the U.S. oil and gas supply chain, *Science*, 361, 186–188, <https://doi.org/10.1126/science.aar7204>, 2018.

760

Enverus | Creating the future of energy together.: <https://www.enverus.com/>, last access: 25 March 2024.

AR6 Synthesis Report: Climate Change 2023: <https://www.ipcc.ch/report/ar6/syr/>, last access: 6 March 2024.

765 MethaneAIR L4 Area Sources 2021 | Earth Engine Data Catalog: https://developers.google.com/earth-engine/datasets/catalog/EDF_MethaneSAT_MethaneAIR_methaneair-L4area-2021, last access: 27 March 2024.



- Brandt, A. R., Heath, G. A., and Cooley, D.: Methane Leaks from Natural Gas Systems Follow Extreme Distributions, *Environ. Sci. Technol.*, 50, 12512–12520, <https://doi.org/10.1021/acs.est.6b04303>, 2016.
- 770 Brantley, H. L., Thoma, E. D., Squier, W. C., Guven, B. B., and Lyon, D.: Assessment of Methane Emissions from Oil and Gas Production Pads using Mobile Measurements, *Environ. Sci. Technol.*, 48, 14508–14515, <https://doi.org/10.1021/es503070q>, 2014.
- Caulton, D. R., Lu, J. M., Lane, H. M., Buchholz, B., Fitts, J. P., Golston, L. M., Guo, X., Li, Q., McSpirtt, J., Pan, D., Wendt, L., Bou-Zeid, E., and Zondlo, M. A.: Importance of Supermitter Natural Gas Well Pads in the Marcellus Shale, *Environ. Sci. Technol.*, 53, 4747–4754, <https://doi.org/10.1021/acs.est.8b06965>, 2019.
- 775 Chan Miller, C., Roche, S., Wilzewski, J. S., Liu, X., Chance, K., Souri, A. H., Conway, E., Luo, B., Samra, J., Hawthorne, J., Sun, K., Staebell, C., Chulakadabba, A., Sargent, M., Benmergui, J. S., Franklin, J. E., Daube, B. C., Li, Y., Laughner, J. L., Baier, B. C., Gautam, R., Omara, M., and Wofsy, S. C.: Methane retrieval from MethaneAIR using the CO₂ Proxy Approach: A demonstration for the upcoming MethaneSAT mission, *EGUsphere*, 1–40, <https://doi.org/10.5194/egusphere-2023-1962>, 2023.
- 780 Chen, Y., Sherwin, E. D., Berman, E. S. F., Jones, B. B., Gordon, M. P., Wetherley, E. B., Kort, E. A., and Brandt, A. R.: Quantifying Regional Methane Emissions in the New Mexico Permian Basin with a Comprehensive Aerial Survey, *Environ. Sci. Technol.*, 56, 4317–4323, <https://doi.org/10.1021/acs.est.1c06458>, 2022.
- 785 Chulakadabba, A., Sargent, M., Lauvaux, T., Benmergui, J. S., Franklin, J. E., Chan Miller, C., Wilzewski, J. S., Roche, S., Conway, E., Souri, A. H., Sun, K., Luo, B., Hawthorne, J., Samra, J., Daube, B. C., Liu, X., Chance, K., Li, Y., Gautam, R., Omara, M., Rutherford, J. S., Sherwin, E. D., Brandt, A., and Wofsy, S. C.: Methane point source quantification using MethaneAIR: a new airborne imaging spectrometer, *Atmospheric Measurement Techniques*, 16, 5771–5785, <https://doi.org/10.5194/amt-16-5771-2023>, 2023.
- 790 Cusworth, D. H., Thorpe, A. K., Ayasse, A. K., Stepp, D., Heckler, J., Asner, G. P., Miller, C. E., Yadav, V., Chapman, J. W., Eastwood, M. L., Green, R. O., Hmiel, B., Lyon, D. R., and Duren, R. M.: Strong methane point sources contribute a disproportionate fraction of total emissions across multiple basins in the United States, *Proceedings of the National Academy of Sciences*, 119, e2202338119, <https://doi.org/10.1073/pnas.2202338119>, 2022.
- Deighton, J. A., Townsend-Small, A., Sturmer, S. J., Hoschouer, J., and Heldman, L.: Measurements show that marginal wells are a disproportionate source of methane relative to production, *Journal of the Air & Waste Management Association*, 70, 1030–1042, <https://doi.org/10.1080/10962247.2020.1808115>, 2020.
- 795 Duren, R. M., Thorpe, A. K., Foster, K. T., Rafiq, T., Hopkins, F. M., Yadav, V., Bue, B. D., Thompson, D. R., Conley, S., Colombi, N. K., Frankenberg, C., McCubbin, I. B., Eastwood, M. L., Falk, M., Herner, J. D., Croes, B. E., Green, R. O., and Miller, C. E.: California’s methane super-emitters, *Nature*, 575, 180–184, <https://doi.org/10.1038/s41586-019-1720-3>, 2019.
- Elvidge, C. D., Zhizhin, M., Baugh, K., Hsu, F.-C., and Ghosh, T.: Methods for Global Survey of Natural Gas Flaring from Visible Infrared Imaging Radiometer Suite Data, *Energies*, 9, 14, <https://doi.org/10.3390/en9010014>, 2016.
- 800 Elvidge, C. D., Baugh, K., Zhizhin, M., Hsu, F. C., and Ghosh, T.: VIIRS night-time lights, *International Journal of Remote Sensing*, 38, 5860–5879, <https://doi.org/10.1080/01431161.2017.1342050>, 2017.
- Fox, T. A., Barchyn, T. E., Risk, D., Ravikumar, A. P., and Hugenholtz, C. H.: A review of close-range and screening technologies for mitigating fugitive methane emissions in upstream oil and gas, *Environ. Res. Lett.*, 14, 053002, <https://doi.org/10.1088/1748-9326/ab0cc3>, 2019.
- 805 de Gouw, J. A., Veeffkind, J. P., Roosenbrand, E., Dix, B., Lin, J. C., Landgraf, J., and Levelt, P. F.: Daily Satellite Observations of Methane from Oil and Gas Production Regions in the United States, *Sci Rep*, 10, 1379, <https://doi.org/10.1038/s41598-020-57678-4>, 2020.
- Jacob, D. J., Varon, D. J., Cusworth, D. H., Dennison, P. E., Frankenberg, C., Gautam, R., Guanter, L., Kelley, J., McKeever, J., Ott, L. E., Poulter, B., Qu, Z., Thorpe, A. K., Worden, J. R., and Duren, R. M.: Quantifying methane



- 810 emissions from the global scale down to point sources using satellite observations of atmospheric methane, *Atmospheric Chemistry and Physics*, 22, 9617–9646, <https://doi.org/10.5194/acp-22-9617-2022>, 2022.
- Johnson, M. R., Tyner, D. R., and Szekeres, A. J.: Blinded evaluation of airborne methane source detection using Bridger Photonics LiDAR, *Remote Sensing of Environment*, 259, 112418, <https://doi.org/10.1016/j.rse.2021.112418>, 2021.
- 815 Kunkel, W. M., Carre-Burritt, A. E., Aivazian, G. S., Snow, N. C., Harris, J. T., Mueller, T. S., Roos, P. A., and Thorpe, M. J.: Extension of Methane Emission Rate Distribution for Permian Basin Oil and Gas Production Infrastructure by Aerial LiDAR, *Environ. Sci. Technol.*, 57, 12234–12241, <https://doi.org/10.1021/acs.est.3c00229>, 2023.
- 820 Lan, X., Talbot, R., Laine, P., and Torres, A.: Characterizing Fugitive Methane Emissions in the Barnett Shale Area Using a Mobile Laboratory, *Environ. Sci. Technol.*, 49, 8139–8146, <https://doi.org/10.1021/es5063055>, 2015.
- Lu, X., Jacob, D. J., Wang, H., Maasackers, J. D., Zhang, Y., Scarpelli, T. R., Shen, L., Qu, Z., Sulprizio, M. P., Nesser, H., Bloom, A. A., Ma, S., Worden, J. R., Fan, S., Parker, R. J., Boesch, H., Gautam, R., Gordon, D., Moran, M. D., Reuland, F., Villasana, C. A. O., and Andrews, A.: Methane emissions in the United States, Canada, and Mexico: evaluation of national methane emission inventories and 2010–2017 sectoral trends by inverse analysis of in situ (GLOBALVIEWplus CH₄ ObsPack) and satellite (GOSAT) atmospheric observations, *Atmospheric Chemistry and Physics*, 22, 395–418, <https://doi.org/10.5194/acp-22-395-2022>, 2022.
- 825 Lu, X., Jacob, D. J., Zhang, Y., Shen, L., Sulprizio, M. P., Maasackers, J. D., Varon, D. J., Qu, Z., Chen, Z., Hmiel, B., Parker, R. J., Boesch, H., Wang, H., He, C., and Fan, S.: Observation-derived 2010–2019 trends in methane emissions and intensities from US oil and gas fields tied to activity metrics, *Proceedings of the National Academy of Sciences*, 120, e2217900120, <https://doi.org/10.1073/pnas.2217900120>, 2023.
- 830 Maasackers, J. D., Jacob, D. J., Sulprizio, M. P., Scarpelli, T. R., Nesser, H., Sheng, J., Zhang, Y., Lu, X., Bloom, A. A., Bowman, K. W., Worden, J. R., and Parker, R. J.: 2010–2015 North American methane emissions, sectoral contributions, and trends: a high-resolution inversion of GOSAT observations of atmospheric methane, *Atmospheric Chemistry and Physics*, 21, 4339–4356, <https://doi.org/10.5194/acp-21-4339-2021>, 2021.
- 835 Miller, S. M., Wofsy, S. C., Michalak, A. M., Kort, E. A., Andrews, A. E., Biraud, S. C., Dlugokencky, E. J., Eluszkiewicz, J., Fischer, M. L., Janssens-Maenhout, G., Miller, B. R., Miller, J. B., Montzka, S. A., Nehr Korn, T., and Sweeney, C.: Anthropogenic emissions of methane in the United States, *Proceedings of the National Academy of Sciences*, 110, 20018–20022, <https://doi.org/10.1073/pnas.1314392110>, 2013.
- 840 Mitchell, A. L., Tkacik, D. S., Roscioli, J. R., Herndon, S. C., Yacovitch, T. I., Martinez, D. M., Vaughn, T. L., Williams, L. L., Sullivan, M. R., Floerchinger, C., Omara, M., Subramanian, R., Zimmerle, D., Marchese, A. J., and Robinson, A. L.: Measurements of Methane Emissions from Natural Gas Gathering Facilities and Processing Plants: Measurement Results, *Environ. Sci. Technol.*, 49, 3219–3227, <https://doi.org/10.1021/es5052809>, 2015.
- 845 Nesser, H., Jacob, D. J., Maasackers, J. D., Lorente, A., Chen, Z., Lu, X., Shen, L., Qu, Z., Sulprizio, M. P., Winter, M., Ma, S., Bloom, A. A., Worden, J. R., Stavins, R. N., and Randles, C. A.: High-resolution U.S. methane emissions inferred from an inversion of 2019 TROPOMI satellite data: contributions from individual states, urban areas, and landfills, *EGUsphere*, 1–36, <https://doi.org/10.5194/egusphere-2023-946>, 2023.
- Ocko, I. B., Sun, T., Shindell, D., Oppenheimer, M., Hristov, A. N., Pacala, S. W., Mauzerall, D. L., Xu, Y., and Hamburg, S. P.: Acting rapidly to deploy readily available methane mitigation measures by sector can immediately slow global warming, *Environ. Res. Lett.*, 16, 054042, <https://doi.org/10.1088/1748-9326/abf9c8>, 2021.
- 850 Omara, M., Sullivan, M. R., Li, X., Subramanian, R., Robinson, A. L., and Presto, A. A.: Methane Emissions from Conventional and Unconventional Natural Gas Production Sites in the Marcellus Shale Basin, *Environ. Sci. Technol.*, 50, 2099–2107, <https://doi.org/10.1021/acs.est.5b05503>, 2016.



- 855 Omara, M., Zimmerman, N., Sullivan, M. R., Li, X., Ellis, A., Cesa, R., Subramanian, R., Presto, A. A., and Robinson, A. L.: Methane Emissions from Natural Gas Production Sites in the United States: Data Synthesis and National Estimate, *Environ. Sci. Technol.*, 52, 12915–12925, <https://doi.org/10.1021/acs.est.8b03535>, 2018.
- Omara, M., Zavala-Araiza, D., Lyon, D. R., Hmiel, B., Roberts, K. A., and Hamburg, S. P.: Methane emissions from US low production oil and natural gas well sites, *Nat Commun*, 13, 2085, <https://doi.org/10.1038/s41467-022-29709-3>, 2022.
- 860 Omara, M., Himmelberger, A., MacKay, K., Williams, J. P., Benmergui, J., Sargent, M., Wofsy, S. C., and Gautam, R.: Constructing a measurement-based spatially explicit inventory of US oil and gas methane emissions, *Earth System Science Data Discussions*, 1–25, <https://doi.org/10.5194/essd-2024-72>, 2024.
- Plant, G., Kort, E. A., Brandt, A. R., Chen, Y., Fordice, G., Gorchov Negron, A. M., Schwietzke, S., Smith, M., and Zavala-Araiza, D.: Inefficient and unlit natural gas flares both emit large quantities of methane, *Science*, 377, 1566–1571, <https://doi.org/10.1126/science.abq0385>, 2022.
- 865 Ravikumar, A. P., Wang, J., McGuire, M., Bell, C. S., Zimmerle, D., and Brandt, A. R.: “Good versus Good Enough?” Empirical Tests of Methane Leak Detection Sensitivity of a Commercial Infrared Camera, *Environ. Sci. Technol.*, 52, 2368–2374, <https://doi.org/10.1021/acs.est.7b04945>, 2018.
- 870 Rella, C. W., Hoffnagle, J., He, Y., and Tajima, S.: Local- and regional-scale measurements of CH₄, δ¹³CH₄, and C₂H₆ in the Uintah Basin using a mobile stable isotope analyzer, *Atmospheric Measurement Techniques*, 8, 4539–4559, <https://doi.org/10.5194/amt-8-4539-2015>, 2015.
- Riddick, S. N., Mauzerall, D. L., Celia, M. A., Kang, M., Bressler, K., Chu, C., and Gum, C. D.: Measuring methane emissions from abandoned and active oil and gas wells in West Virginia, *Science of The Total Environment*, 651, 1849–1856, <https://doi.org/10.1016/j.scitotenv.2018.10.082>, 2019.
- 875 Riddick, S. N., Ancona, R., Mbua, M., Bell, C. S., Duggan, A., Vaughn, T. L., Bennett, K., and Zimmerle, D. J.: A quantitative comparison of methods used to measure smaller methane emissions typically observed from superannuated oil and gas infrastructure, *Atmospheric Measurement Techniques*, 15, 6285–6296, <https://doi.org/10.5194/amt-15-6285-2022>, 2022.
- 880 Riddick, S. N., Mbua, M., Santos, A., Emerson, E. W., Cheptonui, F., Houlihan, C., Hodshire, A. L., Anand, A., Hartzell, W., and Zimmerle, D. J.: Methane emissions from abandoned oil and gas wells in Colorado, *Science of The Total Environment*, 922, 170990, <https://doi.org/10.1016/j.scitotenv.2024.170990>, 2024.
- Robertson, A. M., Edie, R., Snare, D., Soltis, J., Field, R. A., Burkhart, M. D., Bell, C. S., Zimmerle, D., and Murphy, S. M.: Variation in Methane Emission Rates from Well Pads in Four Oil and Gas Basins with Contrasting Production Volumes and Compositions, *Environ. Sci. Technol.*, 51, 8832–8840, <https://doi.org/10.1021/acs.est.7b00571>, 2017.
- 885 Robertson, A. M., Edie, R., Field, R. A., Lyon, D., McVay, R., Omara, M., Zavala-Araiza, D., and Murphy, S. M.: New Mexico Permian Basin Measured Well Pad Methane Emissions Are a Factor of 5–9 Times Higher Than U.S. EPA Estimates, *Environ. Sci. Technol.*, 54, 13926–13934, <https://doi.org/10.1021/acs.est.0c02927>, 2020.
- Rutherford, J. S., Sherwin, E. D., Ravikumar, A. P., Heath, G. A., Englander, J., Cooley, D., Lyon, D., Omara, M., Langfitt, Q., and Brandt, A. R.: Closing the methane gap in US oil and natural gas production emissions inventories, *Nat Commun*, 12, 4715, <https://doi.org/10.1038/s41467-021-25017-4>, 2021.
- 890 Shen, L., Gautam, R., Omara, M., Zavala-Araiza, D., Maasackers, J. D., Scarpelli, T. R., Lorente, A., Lyon, D., Sheng, J., Varon, D. J., Nesser, H., Qu, Z., Lu, X., Sulprizio, M. P., Hamburg, S. P., and Jacob, D. J.: Satellite quantification of oil and natural gas methane emissions in the US and Canada including contributions from individual basins, *Atmospheric Chemistry and Physics*, 22, 11203–11215, <https://doi.org/10.5194/acp-22-11203-2022>, 2022.
- 895 Sherwin, E. D., Rutherford, J. S., Chen, Y., Aminfard, S., Kort, E. A., Jackson, R. B., and Brandt, A. R.: Single-blind validation of space-based point-source detection and quantification of onshore methane emissions, *Sci Rep*, 13, 3836, <https://doi.org/10.1038/s41598-023-30761-2>, 2023.



- 900 Sherwin, E. D., Rutherford, J. S., Zhang, Z., Chen, Y., Wetherley, E. B., Yakovlev, P. V., Berman, E. S. F., Jones, B. B., Cusworth, D. H., Thorpe, A. K., Ayasse, A. K., Duren, R. M., and Brandt, A. R.: US oil and gas system emissions from nearly one million aerial site measurements, *Nature*, 627, 328–334, <https://doi.org/10.1038/s41586-024-07117-5>, 2024.
- 905 Stavropoulou, F., Vinković, K., Kers, B., de Vries, M., van Heuven, S., Korbeń, P., Schmidt, M., Wietzel, J., Jagoda, P., Necki, J. M., Bartyzel, J., Maazallahi, H., Menoud, M., van der Veen, C., Walter, S., Tuzson, B., Ravelid, J., Morales, R. P., Emmenegger, L., Brunner, D., Steiner, M., Hensen, A., Velzeboer, I., van den Bulk, P., Denier van der Gon, H., Delre, A., Edjabou, M. E., Scheutz, C., Corbu, M., Iancu, S., Moaca, D., Scarlat, A., Tudor, A., Vizireanu, I., Calcan, A., Ardelean, M., Ghemulet, S., Pana, A., Constantinescu, A., Cusa, L., Nica, A., Baci, C., Pop, C., Radovici, A., Mereuta, A., Stefanie, H., Dandocsi, A., Hermans, B., Schwietzke, S., Zavala-Araiza, D., Chen, H., and Röckmann, T.: High potential for CH₄ emission mitigation from oil infrastructure in one of EU’s major production regions, *Atmospheric Chemistry and Physics*, 23, 10399–10412, <https://doi.org/10.5194/acp-23-10399-2023>, 2023.
- 910 Thorpe, M. J., Krieting, A., Altamura, D., Dudziak, C. D., Conrad, B. M., Tyner, D. R., Johnson, M. R., Brasseur, J. K., Roos, P., Kunkel, W., Carre-Burritt, A., Abate, J., Price, T., Yaralian, D., Kennedy, B., Newton, E., Rodriguez, E., Elfar, O. I., and Zimmerle, D. J.: Deployment-invariant probability of detection characterization for aerial LiDAR methane detection, 2024.
- 915 Tyner, D. R. and Johnson, M. R.: Where the Methane Is—Insights from Novel Airborne LiDAR Measurements Combined with Ground Survey Data, *Environ. Sci. Technol.*, 55, 9773–9783, <https://doi.org/10.1021/acs.est.1c01572>, 2021.
- Inventory of U.S. Greenhouse Gas Emissions and Sinks: <https://www.epa.gov/ghgemissions/inventory-us-greenhouse-gas-emissions-and-sinks>, last access: 6 March 2024.
- 920 EPA’s Final Rule for Oil and Natural Gas Operations Will Sharply Reduce Methane and Other Harmful Pollution.: <https://www.epa.gov/controlling-air-pollution-oil-and-natural-gas-operations/epas-final-rule-oil-and-natural-gas>, last access: 5 March 2024.
- Weller, Z. D., Hamburg, S. P., and von Fischer, J. C.: A National Estimate of Methane Leakage from Pipeline Mains in Natural Gas Local Distribution Systems, *Environ. Sci. Technol.*, 54, 8958–8967, <https://doi.org/10.1021/acs.est.0c00437>, 2020.
- 925 Williams, J. P., Regehr, A., and Kang, M.: Methane Emissions from Abandoned Oil and Gas Wells in Canada and the United States, *Environ. Sci. Technol.*, 55, 563–570, <https://doi.org/10.1021/acs.est.0c04265>, 2021.
- Williams, J. P., El Hachem, K., and Kang, M.: Controlled-release testing of the static chamber methodology for direct measurements of methane emissions, *Atmospheric Measurement Techniques*, 16, 3421–3435, <https://doi.org/10.5194/amt-16-3421-2023>, 2023.
- 930 Worden, J. R., Cusworth, D. H., Qu, Z., Yin, Y., Zhang, Y., Bloom, A. A., Ma, S., Byrne, B. K., Scarpelli, T., Maasackers, J. D., Crisp, D., Duren, R., and Jacob, D. J.: The 2019 methane budget and uncertainties at 1° resolution and each country through Bayesian integration Of GOSAT total column methane data and a priori inventory estimates, *Atmospheric Chemistry and Physics*, 22, 6811–6841, <https://doi.org/10.5194/acp-22-6811-2022>, 2022.
- 935 Xia, H., Strayer, A., and Ravikumar, A. P.: The Role of Emission Size Distribution on the Efficacy of New Technologies to Reduce Methane Emissions from the Oil and Gas Sector, *Environ. Sci. Technol.*, 58, 1088–1096, <https://doi.org/10.1021/acs.est.3c05245>, 2024.
- Zhang, Y., Gautam, R., Pandey, S., Omara, M., Maasackers, J. D., Sadavarte, P., Lyon, D., Nesser, H., Sulprizio, M. P., Varon, D. J., Zhang, R., Houweling, S., Zavala-Araiza, D., Alvarez, R. A., Lorente, A., Hamburg, S. P., Aben, I., and Jacob, D. J.: Quantifying methane emissions from the largest oil-producing basin in the United States from space, *Science Advances*, 6, eaaz5120, <https://doi.org/10.1126/sciadv.aaz5120>, 2020.



940 Zhou, X., Yoon, S., Mara, S., Falk, M., Kuwayama, T., Tran, T., Cheadle, L., Nyarady, J., Croes, B., Scheehle, E.,
Herner, J. D., and Vijayan, A.: Mobile sampling of methane emissions from natural gas well pads in California,
Atmospheric Environment, 244, 117930, <https://doi.org/10.1016/j.atmosenv.2020.117930>, 2021.

Zimmerle, D., Vaughn, T., Luck, B., Lauderdale, T., Keen, K., Harrison, M., Marchese, A., Williams, L., and Allen,
D.: Methane Emissions from Gathering Compressor Stations in the U.S., *Environ. Sci. Technol.*, 54, 7552–7561,
945 <https://doi.org/10.1021/acs.est.0c00516>, 2020.

950

955